



**UNIVERSITY OF LEEDS**

This is a repository copy of *Can a Computational Model Predict the Effect of Lesion Location on Cam-type Hip Impingement?*.

White Rose Research Online URL for this paper:

<https://eprints.whiterose.ac.uk/195997/>

Version: Accepted Version

---

**Article:**

Jones, AC orcid.org/0000-0002-4984-7507, Stewart, TD orcid.org/0000-0002-6868-9938, Maher, N et al. (1 more author) (2023) Can a Computational Model Predict the Effect of Lesion Location on Cam-type Hip Impingement? *Clinical Orthopaedics and Related Research*. ISSN 0009-921X

<https://doi.org/10.1097/corr.0000000000002565>

---

© 2023 by the Association of Bone and Joint Surgeons. This is an author produced version of an article published in *Clinical Orthopaedics and Related Research*. Uploaded in accordance with the publisher's self-archiving policy.

**Reuse**

Items deposited in White Rose Research Online are protected by copyright, with all rights reserved unless indicated otherwise. They may be downloaded and/or printed for private study, or other acts as permitted by national copyright laws. The publisher or other rights holders may allow further reproduction and re-use of the full text version. This is indicated by the licence information on the White Rose Research Online record for the item.

**Takedown**

If you consider content in White Rose Research Online to be in breach of UK law, please notify us by emailing [eprints@whiterose.ac.uk](mailto:eprints@whiterose.ac.uk) including the URL of the record and the reason for the withdrawal request.



[eprints@whiterose.ac.uk](mailto:eprints@whiterose.ac.uk)  
<https://eprints.whiterose.ac.uk/>

## Can a computational model predict the effect of lesion location on cam-type hip impingement?

Alison C. Jones PhD<sup>1</sup>, Todd D. Stewart PhD<sup>1</sup>, Niall Maher MSc<sup>2</sup>, Colin Holton FRCS, MSc, MBChB<sup>2,3</sup>

<sup>1</sup>Leeds Institute of Medical and Biological Engineering, University of Leeds, UK

<sup>2</sup>Leeds Teaching Hospitals NHS Trust, Leeds, UK

<sup>3</sup>National Institute for Health Research Leeds Biomedical Research Centre, Leeds, UK

The institution of one or more of the authors (ACJ) has received, during the study period, funding from the Royal Academy of Engineering under the Leverhulme Trust Research Fellowship scheme. The institution of one or more of the authors (CH) has received, during the study period, funding from the National Institute for Health Research Leeds Biomedical Research Centre.

All ICMJE Conflict of Interest Forms for authors and *Clinical Orthopaedics and Related Research*<sup>®</sup> editors and board members are on file with the publication and can be viewed on request.

Ethical approval was not sought for the present study.

This work was performed at the School of Mechanical Engineering, University of Leeds, Leeds, UK.

A. Jones ✉

Leeds Institute of Medical and Biological Engineering, School of Mechanical Engineering, Woodhouse Lane, University of Leeds, LS2 9JT, UK

[a.c.jones@leeds.ac.uk](mailto:a.c.jones@leeds.ac.uk)

## **Abstract**

*Background* The Warwick consensus defined femoroacetabular impingement syndrome (FAIS) as a motion-related clinical disorder of the hip with a triad of symptoms, clinical signs and imaging findings, representing symptomatic premature contact between the proximal femur and the acetabulum. Several factors appear to affect the labral and cartilage damage caused, including joint shape and orientation, and patient activities. There is a lack of tools to predict impingement patterns in an individual patient across activities. Current computational modelling tools either measure pure range of motion of the joint or include complexity which reduces reliability and increases time to achieve a solution.

*Questions/purposes* The purpose of this study was to examine the efficacy of a low computational cost approach to combining cam-type hip shape and multiple hip motions for impingement prediction. Specifically, we sought to determine 1) the potential to distinguish impingement from individual hip shapes by analyzing the difference between a cam lesion located at the anterior and one located at the superior of the femoral neck; 2) the sensitivity to three aspects of hip alignment, namely femoral neck-shaft angle, femoral version angle and pelvic tilt; and 3) the difference in impingement measures between the individual activities in our hip motion dataset.

*Methods* A model of the shape and alignment of a cam-type impinging hip was created and used to describe two locations of a cam lesion on the femoral head-neck junction (superior and anterior) based on joint shape information available in prior studies. Sensitivity to hip alignment was assessed by varying three aspects from a baseline (a typical alignment described in prior studies), namely femoral neck-shaft angle, femoral version, and pelvic tilt. Hip joint movements were selected from an existing database of 18 volunteers performing 13 activities (10 males, 8 females, age  $44 \pm 19$  years). A subset was selected, aiming to maximise variation in the range of joint angles and maintain a consistent number of people

performing each activity, which resulted in nine people per activity, including at least three of each sex. Activities included a pivot during walking, a squat and a golf swing. All selected hip joint motion cases were applied to each hip shape model. For the first part of the study, the number of motion cases where impingement was predicted (impingement rate) was recorded. Quantitative analysis of the depth of penetration of the cam lesion into the acetabular socket and qualitative observations of impingement location were made for each lesion location (anterior and superior). In the second part, which aimed to test the sensitivity of the findings to hip joint orientation, the full analysis of both cam lesion locations was repeated for three modified joint orientations. Finally, the results from the first part of the analysis were divided by activity, in order to understand how the composition of the activity dataset affected the results.

*Results* The two locations of cam lesion generated different rates of impingement (anterior cam - 56% of motion cases, superior cam - 13% of motion cases), and different areas of impingement within the acetabular, but similar penetration depths (anterior cam  $6.8^{\circ} \pm 5.4^{\circ}$ , superior cam  $7.9^{\circ} \pm 5.8^{\circ}$ ). The most substantial effects of changing the joint orientation were: lowering the femoral version angle for the anterior cam, which increased the impingement rate to 67%; and lowering the neck-shaft angle for the superior cam, which increasing the impingement rate to 36%. Flexion-dominated activities only generated impingement with the anterior cam (for example, the squat). The superior cam generated impingement during activities with high internal-external rotation of the joint (for example, the golf swing).

*Conclusion* This work has demonstrated the capability of a simple, rapid computational tool for assessing impingement of a specific cam-type hip shape. It is the first to do so over a large set of motion cases, representing a range of activities affecting the hip joint, and has potential for use in planning of surgical bone removal.

*Clinical Relevance* The results of this study imply that FAIS patients with cam lesions on the superior femoral head-neck junction may impinge during motions which are not strongly represented by current physical diagnostic tests.

## Introduction

The Warwick consensus defined femoroacetabular impingement syndrome (FAIS) as a motion-related clinical disorder of the hip with a triad of symptoms, clinical signs and imaging findings, representing symptomatic premature contact between the proximal femur and the acetabulum [14]. Cam-type FAIS is characterized by an out-of-round femoral head shape [12, 25] and the presence of a lesion on the femoral side has been correlated with damage to the acetabular cartilage [2, 4]. The mechanism of impingement has been described as the movement of the cam lesion into the acetabular socket [4, 38]. Sporting activities which include extremes of hip joint motion, particularly in flexion and internal-external rotation, are associated with increased occurrence of FAIS [1, 41, 39], and clinical diagnostic tests replicate large flexion angles or modified internal-external rotation [7]. The surgical intervention which includes the removal of those out-of-round parts of the femoral head-neck junction [5, 6] has shown good results in reducing hip pain, with some benefit over conservative treatment [15, 31].

The diagnosis and treatment of cam-type FAIS are complex because the radiographic features used to indicate the presence of a cam-type femur are also present in the asymptomatic population [13, 26] and the patient-specific impingement mechanism is not easy to discern. Although particular movements are linked to hip impingement, we currently lack the ability to assess the mechanism and severity of impingement over a range of different activities for the hip joint shape of an individual. Computational modelling methods exist which can be used to predict pressures at the cartilage labral junction with cam-type hip shapes [28], however these models are challenging and time consuming to conduct in a patient-specific manner. Even where the shape modelling is partially automated [9], achieving a reliable solution can be challenging and computationally intensive, with solution time of 1-3 hours for

90° flexion and 35° internal rotation for one hip shape [8]. These challenges limit the number of joint motion cases that can be performed.

The purpose of this study was to examine the efficacy of a low computational cost approach to combining cam-type hip shape and multiple hip motions for impingement prediction. Specifically, we sought to determine 1) the potential to distinguish impingement in individual hip shapes by analyzing the difference between a cam lesion located at the anterior and one located at the superior of the femoral neck; 2) the sensitivity to three aspects of hip alignment, namely femoral neck-shaft angle, femoral version angle and pelvic tilt; and 3) the difference in impingement measures between the individual activities in our hip motion dataset.

## **Materials and Methods**

### *Overview of Study Design*

To address our study aims, we created a computational model of interarticular impingement in cam-type hip joints where individual features of bony shape and joint alignment could be independently adjusted. A range of possible hip motions were selected from an existing database. Each hip shape was combined with each hip motion and the presence or absence of impingement was recorded, along with the maximum depth of penetration of the cam lesion past the acetabular rim. These measures were then summarized over the motion cases performed to provide measures of the potential for impingement for one hip shape case (Fig. 1). To assess the potential to distinguish impingement from individual hip shapes, we compared the measures of impingement between a cam lesion located at the anterior and one located at the superior of the femoral neck. Hip motion data from nine volunteers performing 13 activities were applied to each hip shape and measures of impingement severity were

recorded. To assess the sensitivity to femoral neck-shaft angle, femoral version angle and pelvic tilt, those three joint orientation angles were adjusted from a typical baseline value by the same amount each. The full analysis over both hip shape cases and all motion cases (combinations of volunteers and activities) was repeated for each adjusted joint alignment, and the same set of impingement measures were recorded. To investigate the difference in impingement severity between the individual activities in our hip motion dataset, the measures recorded in the first part of the study were broken down by activity.

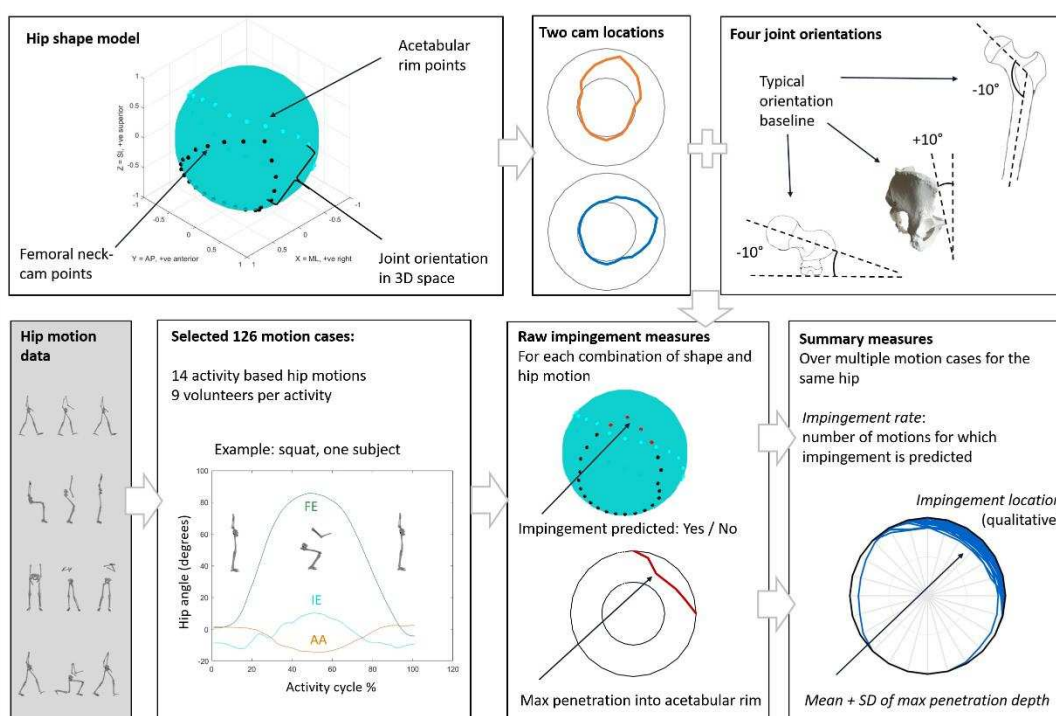


**Fig. 1** A flow diagram illustrating: the shape model and the shape cases generated for the study; the hip motion database and subset selected; the raw measures taken for each combination of hip shape and motion; and the summary measures taken over the relevant motion cases for each hip shape.

### *Motion Data and Volunteers*

Relative hip angles in three planes were calculated as part of a previous project [21, 22]. A 13-camera Qualysis Oqus 3D motion capture system (Qualisys™ Medical AB) was used to collect skin marker motion data for 18 people (10 males, 8 females, age  $44 \pm 19$  years) and 13 activities, and processed to generate hip joint angles. Volunteers were recruited from the general population and were free from any conditions affecting their mobility [22]. Five trials were collected for each subject performing each activity. Hip angles were calculated in Visual3D software (C-Motion Inc), and some trials were unsuccessful due to lack of marker visibility. In the current study, the complete set of data was analysed to find hip motion cases with the highest and lowest hip rotation angles in each plane. A smaller dataset was then selected with the aims of including the same number of volunteers for each activity, including one trial per person, and representing the highest and lowest hip rotations from the wider dataset. This resulted in data from nine people for each activity, where the specific people selected for each activity were slightly different. The activities were: (1) level walking; (2) a step onto the right leg and pivot to the left; (3) walking on an inclined surface; (4) walking in a declined surface; (5) stand to sit; (6) sit to stand; (7) crossing right ankle over the left leg while seated; (8) squat; (9) standing forward bend, reaching towards the ground; (10) reaching forward in a kneeling position; (11) a lunge with the right leg forwards; (12) a golf swing; and (13) cycling. Data were analysed for one hip in twelve of the activities. The step-pivot, seated leg cross and lunge activities were performed on the right side and therefore the right hip was used. For the golf swing, both the leading and trailing hips were analysed separately, resulted in a total of 14 hip activity-based hip movements. The hip angles from this envelope of 14 activity-based movements from nine different people were used for the study (in total 126 motion cases). Motions from least three people of each sex were selected

for each activity-based movement and, of the overall 126 motion cases, 61 were from males and 65 from females.

Complete hip motion and force data from the previous project are available in an open dataset [37] and the subset is described in full in the open dataset associated with this study [17].

### *Hip Shape Model*

A set of points was defined in 3D space to describe the location of the inner edge of the cam morphology and the start of the femoral neck (Fig. 2A-B) and a second set of points was defined to describe the acetabular bony rim. The modelling assumption was that if any of the cam edge points passed over the acetabular rim during an activity, impingement had been initiated.

A baseline set of points representing the shape of a normal femoral neck, in the absence of a cam, were created based on data from Nakahara et al. [27]. Twenty-four points were evenly distributed around the femoral neck and their positions defined by the line connecting the point to the femoral head center and its angle with the femoral neck direction. Information on the location and extent of cam morphologies was used to generate the cam shape cases (Fig. 2C-D). The location of the highest alpha angle is consistently reported to be between the superior and the anterior of the femoral neck [11, 23]. The final set of “cam-neck” points for each hip shape represented the edge of the cam lesion and, away from that lesion, they represented the edge of the femoral neck. Cam shape cases included a superior location, where the highest alpha angle was located at the 12:30 clock face position and an anterior location (at 02:30). In both cases a large cam was replicated, with a maximum alpha angle of  $80^\circ$  [34, 40]. We used prior studies on the extent of cam morphologies around the sagittal circumference of the head [26, 40] to scale the cam extent in line with the selected maximum

alpha angle. Initially the cam-neck points were defined in a local coordinate system aligned with the femoral neck.

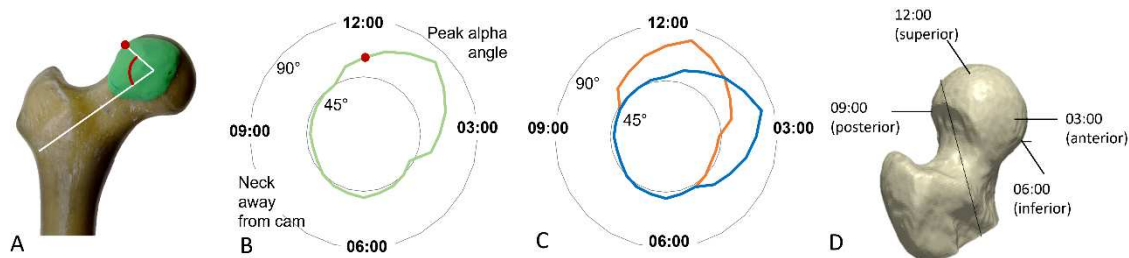


**Fig. 2** (A) An illustration of one of the angles used to define a neck-cam edge point (red dot); the angle between a line along the femoral neck and a line from the femoral head center to cam edge (equivalent to a clinical alpha angle, red curve). A right proximal femur is depicted. (B) A clock face representation of the 24 cam-neck edge points used in the shape model (points connected with a green line). Where there is a cam lesion, the radial angle depicts an alpha angle (red dot = superior alpha angle matching illustration A). Away from the cam lesion the radial angle represents the start of the femoral neck. (C) The two cam location cases used in this study (orange line = superiorly located cam, blue line = anteriorly located cam). (D) An illustration of the clockface notation used in the plots, including anatomic orientation.

The set of points describing the location of the bony acetabular rim was defined in a local coordinate system aligned with the acetabular rim plane outward facing normal vector (Fig. 3A). In this study, the acetabular points represented the location of a typical acetabular rim shape from a control population (Fig. 3B), defined based on prior studies [18, 36].

For the definition of femoral and acetabular point sets, data was taken from studies with measurements of greater than 40 patients (or bones) and the values extracted were verified using at least one additional source.

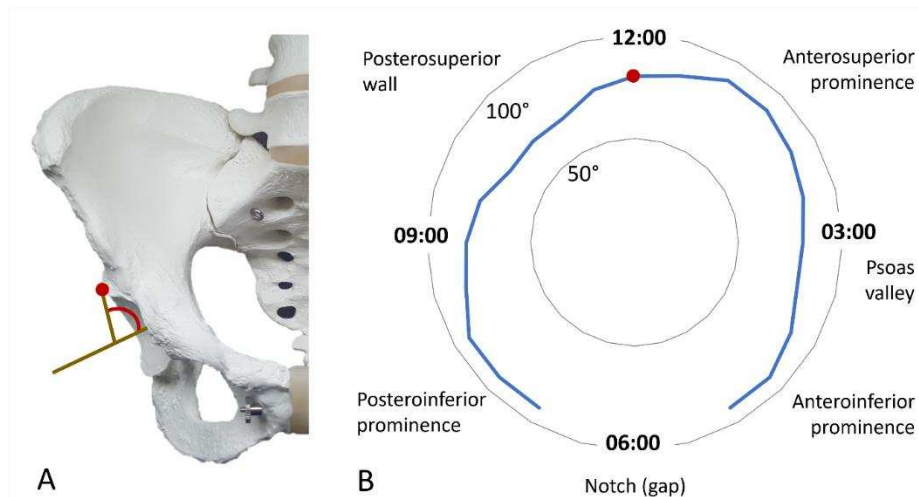


**Fig. 3** (A) An illustration of one of the angles used to define an acetabular rim point (red dot); the angle between the acetabular rim plane outward facing normal vector and a line connecting the socket center to the relevant acetabular rim point (red curve). (B) A clock face representation of the 21 acetabular rim point angles used in the shape model (points connected with blue line, red dot = superior point matching illustration A).

We defined the baseline hip alignment in a neutral standing position with a set of bony alignment measures (Fig. 4). The acetabular inclination ( $50^\circ$ , equivalent to a Centre Edge angle of  $40^\circ$ ), version ( $16^\circ$ ), and tilt ( $19^\circ$ ) defined within the pelvis, were taken close to the mean of several anatomical studies [13, 16, 18, 24]. Each of the hip orientation angles for the baseline case were approximations of the mean from both FAIS and control populations, namely: a femoral neck-shaft angle of  $125^\circ$  [16, 27, 35], a femoral neck version of  $15^\circ$  [13, 23, 27], and a pelvic tilt of  $-2^\circ$  [33, 42]. These measures were combined to define the orientation of the cam-neck points and the acetabular points within a shared coordinate system.

Complete details and algorithms for the hip shape model are provided in an open dataset [17].

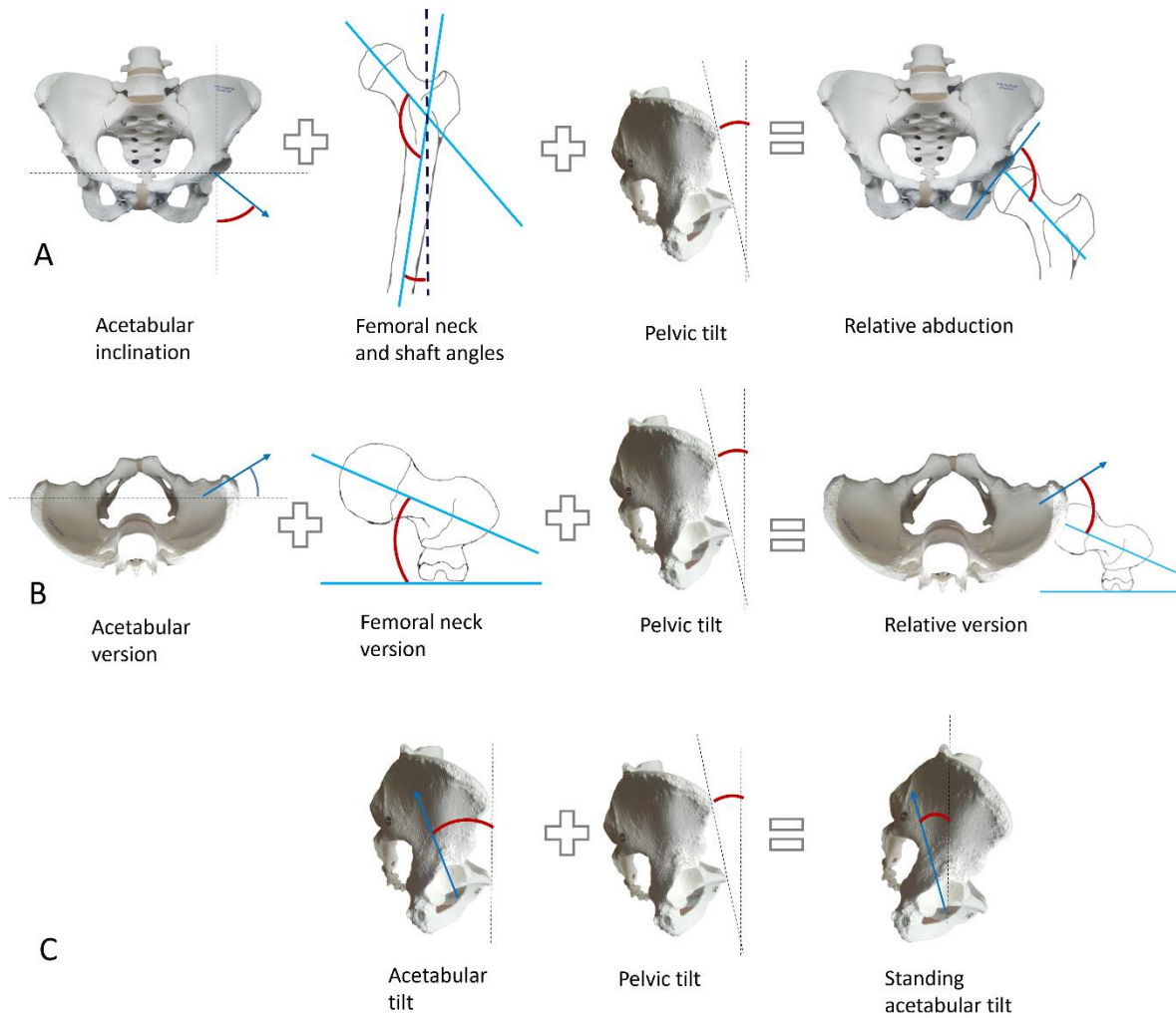


**Fig. 4** The relative orientation of the acetabular and the femoral sides. (A) The combination of acetabular inclination, femoral neck angle, and pelvic tilt defines the relative abduction of the joint. (B) The combination of acetabular version, femoral neck version, and pelvic tilt defines the relative version of the joint. (C) Acetabular tilt (within the pelvis) and pelvic tilt combine to generate the effective acetabular tilt in a standing position. Blue lines provide an indication of the reference lines used to take angular measurements (red curves).

### *Contact Algorithm and Metrics*

We developed algorithms in Matlab (R2020a The Mathworks Inc) to define the sets of cam-neck and acetabular points, align the hip in a neutral standing position, and apply the joint angle data from the 126 motion cases through each point in the activity cycles. Motion cases in which the cam-neck points had moved past the acetabular rim were identified. The impingement rate was defined as the number of motion cases in which impingement was predicted and gave an indication of the likelihood of impingement for that hip shape. During motion cases where impingement occurred, the greatest angular overlap between the cam lesion and the acetabular rim was recorded at each point around the acetabular. This data was plotted to show the angular depth of impingement into the acetabulum at each position around the rim. (The lines on these plots can be thought of as tide marks, showing the extent of penetration of the cam into the acetabular over the whole motion.) Plots of acetabular penetration depth were overlaid for all motion cases and used to qualitatively establish the dominant location of impingement for each hip shape. The maximum acetabular penetration depth from anywhere around the rim was recorded for each motion case. The acetabular penetration depth data are given as angles, independent of hip joint size. For context, they are also given in millimeters, based on the assumption of an acetabular socket radius of 25 mm.

### *Ethical Approval*

Ethical approval was not sought for the present study.

### *Statistical Analyses*

We used the large superior and large anterior cam shape cases in combination with all 126 motion cases to observe differences in impingement rate, acetabular impingement location, and penetration depth between the two cam locations. The impingement rate was therefore a

number out of 126. The mean and standard deviation of the maximum acetabular penetration depth were taken over all the motion cases in which impingement was predicted for each hip shape.

The initial analysis was then repeated for three adjustments to the hip orientation representing a change of 10° in each of the femoral neck shaft angle, femoral version angle, and pelvic tilt.

The adjusted hip orientation values represented: a coxa vara hip with a neck-shaft angle of 115° [23, 30], a low femoral version angle of 5° [23], and an anterior pelvic tilt of 8°, within normal range [33, 42]. Each of these orientation changes make a difference to the overall clearance in the joint in each plane. Angles indicating those changes are given in Table 1.

Observations were made about the relative effect of these changes in joint orientation on the impingement rate and penetration depth measures.

Finally, we analysed the impingement rate and acetabular penetration depth for each of the 14 hip activities separately. In this case the impingement rate for each combination of hip shape and activity was reported out of the nine people performing that activity. The mean and standard deviation of the maximum acetabular penetration depth were calculated over the subset of those nine cases where impingement occurred. Where the number of people predicted to impinge was less than three, the penetration depth data was not included.

**Table 1.** Description of the four hip orientation cases in terms of the relative joint orientation in each plane. Values given in bold indicate deviations from the baseline case, where the change in angle given in the case description has generated a change in relative angle in one or more plane.

Hip joint orientation case	Relative abduction	Relative version	Acetabular tilt
Baseline	91°	33°	21°
Low femoral neck-shaft angle (115°)	<b>81°</b>	33°	21°
Low femoral neck version (5°)	91°	<b>23°</b>	21°
Anterior pelvic tilt (8°)	<b>90°</b>	<b>25</b>	<b>11°</b>

## Results

### *Distinguishing Impingement between Anterior and Superior Cam Lesions*

The two locations of cam lesion generated different rates of impingement, and different areas of impingement within the acetabular, but similar penetration depths into the acetabular. Qualitatively, the predicted impingement was focused in the superior-posterior acetabulum for the superior cam hip and superior-anterior for the anterior case (Fig. 5, Baseline). A high impingement rate was predicted for the anterior cam (56% [71 of 126] of motion cases) compared with the superior cam (13% [17 of 126]). The mean  $\pm$  SD of penetration depth over the motion cases were similar in the superior cam ( $7.9^\circ \pm 5.8^\circ$ ) and anterior cam ( $6.8^\circ \pm 5.4^\circ$ ) cases.

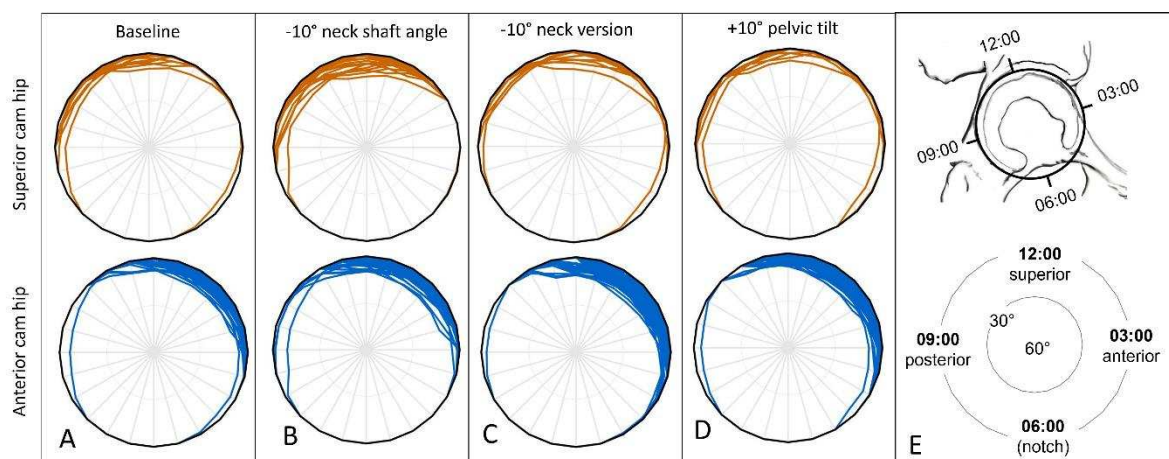


**Fig. 5** Maps of impingement location and penetration depth experienced on the acetabular rim for (A) the baseline hip joint orientation, (B) a low neck-shaft angle, (C) a low femoral version angle, (D) an anterior pelvic tilt. Each coloured line represents the extent of impingement through a single motion case (orange lines = superior cam cases, blue line = anterior cam cases). (E) Schematics providing the anatomical orientation of the clockface plots and angular scale (e.g. the number of degrees by which the cam overlapped with the acetabular at that position).

### *Assessing the Sensitivity to Hip Orientation*

Varying the joint orientation generated different effects for the anterior versus the superior cam lesion (Fig. 5, Table 2). For the anterior cam, all orientation changes increased the mean penetration depth and increased the number of motion cases where impingement was predicted. The effect was most pronounced when lowering the femoral version angle, which generated impingement in an additional 13 motion cases (increasing the impingement rate to 67%) and increasing the mean penetration depth by 5° (or 2 mm). For the superior cam hip, lowering the neck-shaft angle had the most pronounced detrimental effect, more than doubling the impingement rate (from 17 to 46, increasing the impingement rate to 36%), but with very little effect on the mean penetration depth (a change of 2° or less than 1 mm).

**Table 2.** Rate of impingement and acetabular penetration depth for all cam location and joint orientation cases. Impingement rate is the number of motion cases where impingement was predicted, out of 126 motion cases (14 hip movements, nine subjects). Acetabular penetration depth is given as the mean  $\pm$ SD over all motion cases where impingement was predicted. The measure in degrees is independent of joint size and the equivalent in millimeters is calculated by assuming an acetabular socket radius of 25 mm.

Cam location case		Superior			Anterior		
Impingement measurement		Rate	Depth in °	Depth in mm	Rate	Depth in °	Depth in mm
Joint orientation cases	Baseline	17	8 $\pm$ 6	3 $\pm$ 3	71	7 $\pm$ 5	3 $\pm$ 2
	-10° neck shaft angle	46	6 $\pm$ 8	3 $\pm$ 3	79	8 $\pm$ 6	3 $\pm$ 3
	-10 femoral version	26	6 $\pm$ 6	2 $\pm$ 2	84	12 $\pm$ 7	5 $\pm$ 3
	+10° pelvic tilt	21	6 $\pm$ 5	2 $\pm$ 2	77	9 $\pm$ 6	4 $\pm$ 3

*Establishing the Difference in Impingement Between Activities*

Analysing the results at an individual activity level showed that the activities which generated impingement for the anterior cam were somewhat distinct from those which generated impingement for the superior cam (Table 3). Flexion-dominated activities such as sit to stand, squat and reaching forward in a kneeling position, only generated impingement with the anterior cam. Impingement was predicted for all nine people performing these activities in combination with an anterior cam and that impingement was located in the superior-anterior section of the acetabular rim (Fig. 6). The superior cam generated impingement during the walking pivot, leg cross while seated, the golf swing (both leading and trailing hips) and during cycling. Those activities are typically characterized by higher internal-external rotation of the joint. Impingement was typically in the superior or superior-posterior areas of the acetabular. Activities that caused impingement with the superior cam also caused some impingement for the anterior cam. No impingement was seen for either cam location for the walk or decline walk activities.

The activity with the highest mean penetration depth was for the golf swing leading hip (13° or 6 mm) and the lowest was for cycling (2° or 1 mm), both in combination with a superior cam. The mean penetration depth was more consistent across activities for the anterior cam, ranging between 3° and 9° (or 1-4 mm).

**Table 3.** The rate of impingement and acetabular penetration depth for each individual activity. Impingement rate is the number of subjects for whom impingement was predicted, out of the nine subjects performing each activity. Acetabular penetration depth is given as the mean  $\pm$  SD over all subjects where impingement was predicted. The measure in degrees is independent of joint size and the equivalent in millimeters is calculated by assuming an acetabular socket radius of 25 mm. The depth measure is only provided where the three or more subjects were predicted to impinge.

	Cam location case	Superior			Anterior		
		Rate	Depth in $^{\circ}$	Depth in mm	Rate	Depth in $^{\circ}$	Depth in mm
Activity	Walk pivot	1			1		
	Incline walk	0			1		
	Stand to sit	0			9	4 $\pm$ 4	2 $\pm$ 2
	Sit to stand	0			9	7 $\pm$ 3	3 $\pm$ 2
	Cross leg	3	6 $\pm$ 4	3 $\pm$ 2	9	8 $\pm$ 7	3 $\pm$ 3
	Squat	0			9	8 $\pm$ 5	4 $\pm$ 2
	Forward bend	0			6	3 $\pm$ 4	1 $\pm$ 2
	Kneel reach	0			9	8 $\pm$ 4	3 $\pm$ 2
	Lunge (leading)	0			3	8 $\pm$ 4	4 $\pm$ 2
	Golf (leading)	6	13 $\pm$ 6	6 $\pm$ 3	5	9 $\pm$ 7	4 $\pm$ 3
	Golf (trailing)	4	7 $\pm$ 3	3 $\pm$ 1	2		
	Cycle	3	2 $\pm$ 3	1 $\pm$ 1	8	6 $\pm$ 6	3 $\pm$ 2

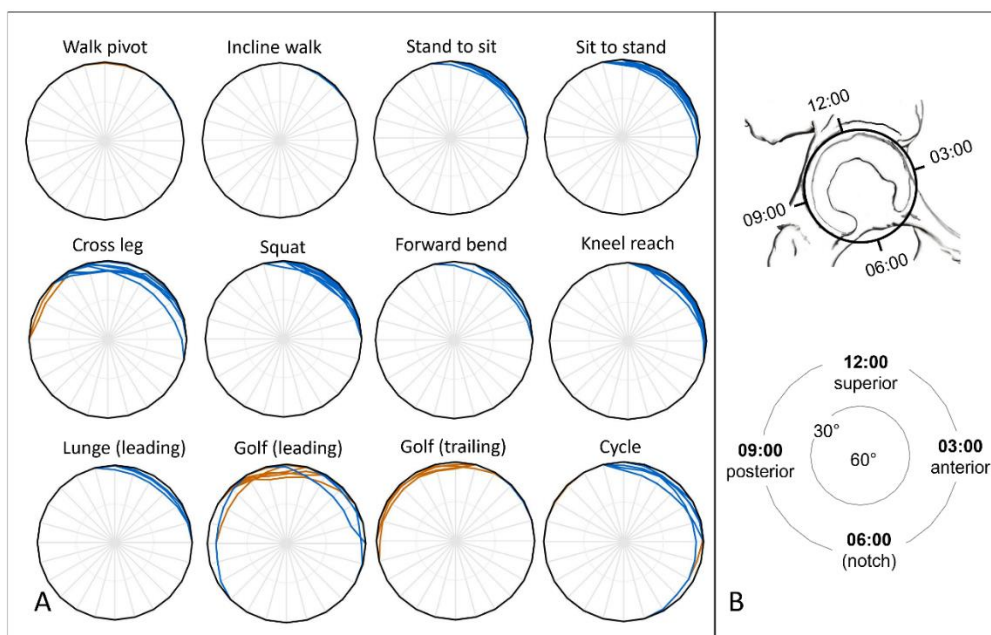


**Fig. 6** (A) Maps of impingement location and penetration depth experienced on the acetabular rim, for each of the activities tested. Each coloured line represents the extent of impingement through a single motion case (orange lines = superior cam cases, blue line = anterior cam cases). (B) Schematics providing the anatomical orientation of the clockface plots and angular scale (e.g. the number of degrees by which the cam overlapped with the acetabular at that position).

## Discussion

Cam-type and mixed-type FAIS have been associated with damage to the articular cartilage as well as the labrum and this type of extensive damage is challenging to manage surgically. The variation from patient to patient in three-dimensional shape of hip, and nature of activities undertaken regularly, pose a challenge when assessing the severity of impingement. Improvements in the clarity of this individual assessment would enhance both the selection of candidates for surgery and the surgical bone resection plan. The ability to use computational models for this purpose is limited by the requirement for an expert user to problem solve unreliable solution processes, and the time taken to compute solutions. Using a typical finite element model calculation of impingement in combination with the 126 cases in this study would take over 5 days to complete. This work has demonstrated the potential of a shape-motion model for the prediction of cam-type hip impingement over a range of activities, with robust solution and a total solution time of less than 5 mins. Results demonstrating the interaction between shape and orientation are aligned with current understanding and provide some confidence in the model. The low penetration depth of the cam into the acetabulum has implications for the mechanism of cartilage damage. The ability to identify specific activities which generate high rates of impingement for different cam-lesion locations, has potential for use in the clinical evaluation of patients with hip pain. To realise the benefit of this computational tool in clinical practice, the next steps are to apply the shape model to individual FAIS patients, to streamline the extraction of shape data from imaging, and to use the model's flexibility to understand the importance of individual features of their joint shape to the impingement experienced.

### *Limitations*

This study has limitations. The shape model currently captures only the leading edge of the cam lesion. The shape of the cam surface beyond the leading edge is likely to affect impingement severity, with cam lesions protruding further outside the best fit sphere of the femoral head having a greater potential for damage [10, 11]. This aspect is currently not captured within the model and is an area for future development. In this study, only hip motion was considered and not the joint contact forces. An activity with a large impingement penetration depth may not cause tissue damage in the absence of a high joint contact force. The ‘seated leg cross’ activity may well fall in that category.

The hip motion data used in this study were taken from volunteers from the general population. This choice has the advantage of representing pain-free joint function, indicative of early tissue damage conditions, rather than the more limited motion seen in those with symptomatic FAIS [3, 20]. A disadvantage of this approach is that some individual motion cases will be a poor match for the simulated hip anatomy, perhaps creating an unrealistic level of impingement. Therefore, any analysis should consider the possibility of unrealistic outliers in the results. The selection of activities does not account for different motion types or the frequency of different activities, and some motion characteristics of the hip may not be represented. Currently, the dataset includes a large proportion of flexion-dominated hip motions (7 of 13) that were shown to generate impingement preferentially with anteriorly located cams, over superiorly located cams. Hip motion is indeed flexion dominated and therefore this does not seem unreasonable; however, these relative impingement rate values should be interpreted with care.

The model is representative of only the bony features of the joint, neglecting the soft tissues. Therefore, the potential for soft tissue damage through restriction of the joint space during impingement is considered, but predictions of the soft tissue deformation or pressure are not.

Equally the stability (or instability) of the joint due to capsular and ligament tissues are not considered. These simplifications eliminate the possibility of the solution process failing and significantly reduce solution times. This approach has overlap with those used to measure joint range of motion using CT-based solid modelling approaches for cam-type hips, where potential targets for bone removal can be indicated [19]. The ability in this work to rapidly apply a large envelope of activity-based motions and track impingement depth extends that capability.

While the results presented here are logical and match previously reported correlations between hip shape and damage types, this provides only a partial validation of the model at the broad population level. Work remains to be done in validating the predictions against labral and cartilage damage seen in individual patients, and in understanding the precision of shape capture and motion dataset needed to achieve that individual prediction.

### *Discussion of Key Findings*

Results presented here have demonstrated an ability to assess impingement location and severity for combinations of cam lesion positions and hip joint orientations, across multiple activities. Logical results in terms of the combination of joint angles and cam locations, along with correspondence of findings with existing understanding, provide confidence in the tool. The most common cam lesion location is in the anterior-superior area of the head-neck junction [11, 34] and the anterior-superior area of the acetabulum is the most common location for tissue damage [32]. The difference in impingement location for the anterior and superior cam hips in this work show that the location of the greatest damage may be predictable for an individual. Hip alignment has been shown to affect the impingement risk [23], which is consistent with the effect on impingement rates being different for the anterior

cam compared with the superior cam. With a baseline level of confidence in the tool, the aims of application to individual patient data can be pursued.

None of the mean penetration depths recorded in this work would extend beyond the first third of the acetabular cartilage (Table 2). That implies that a cam lesion would need to have a maximum alpha angle of greater than  $80^{\circ}$  to directly restrict the joint space beyond the first third of the lunate cartilage surface, in the activities tested. If the recorded penetration depths were assumed to directly translate to the extent of cartilage damage, they would all fall within the lowest cartilage damage extent category which is recorded in the UK Non-Arthroplasty Hip Registry [29]. The recorded depths are under half of the mean cartilage damage depth recorded for isolated cam lesions by Beck et al [4]. This finding strengthens the evidence that cartilage damage occurring further into the joint is generated by a secondary damage mechanism, such as the shearing of the cartilage away from the bone after initial damage to the cartilage-labral junction [4].

This work has demonstrated that the number of activities where impingement occurs between the cam and the acetabular rim is more limited for a lesion on the superior of the head-neck junction versus one on the anterior (Table 3). This may have implications for the clinical assessment of patients with a symptomatic hip and a superiorly located lesion. A combination of clinical diagnostic tests have been recommended to improve the chance of detecting an impinging hip [7], including a progression of flexion, adduction, and internal rotation (FADIR), foot progression angle walking (FPAW) and maximal squat. The current data implies that activities with a large amount of internal rotation of the hip (such as a golf swing) are more likely to cause impingement for these patients than activities with high flexion (such as a squat). Larger internal rotations in the absence of flexion may not be captured in clinical assessment, with the potential to miss some impingement with superiorly located lesions.

### *Conclusion*

This work has demonstrated the capability of a simple, rapid computational tool for opening up our understanding of how the combination of multiple bony shape features and motions during activities influence impingement in the hip joint. Insight into the likely depth of penetration of a cam lesion into the acetabular under multiple activities contributes to our scientific understanding of the mechanism of cartilage damage. The ability to establish which activities are more relevant to impingement for different locations of cam lesion provides insight which can be incorporated into the clinical evaluation of patients.

The more ambitious use of the tool for planning of surgical bone removal will require the streamlining of patient-specific shape extraction from imaging, model sensitivity testing, evaluation and possibly expansion of the hip activity database, as well as validation of the impingement predictions at an individual patient level. These aspects will form the next stage of this work.

### **Acknowledgments**

We thank Prof. Tim Board, of the Centre for Hip Surgery at Wrightington Hospital, and Prof. Sophie Williams, of the School of Mechanical Engineering at the University of Leeds, for their discussion of, and suggestions for, this work.

## References

1. Agricola R, Heijboer MP, Ginai AZ, et al., A cam deformity is gradually acquired during skeletal maturation in adolescent and young male soccer players: a prospective study with minimum 2-year follow-up. *Am J Sports Med.* 2014;42:798–806
2. Anderson LA, Peters CL, Park BB, et al., Acetabular cartilage delamination in femoroacetabular impingement, *J Bone Joint Surg Am.* 2009;91:305-13
3. Bagwell JJ, Snibbe J, Gerhardt M, et al., Hip kinematics and kinetics in persons with and without cam femoroacetabular impingement during a deep squat task, *Clin Biomec (Bristol Avon).* 2016;31:87-92.
4. Beck M, Kalhor M, Leunig M, et al., Hip morphology influences the pattern of damage to the acetabular cartilage: femoroacetabular impingement as a cause of early osteoarthritis of the hip. *J Bone Joint Surg Br.* 2005;87:1012–1018
5. Beck M, Leunig M, Parvizi J, et al., Anterior femoroacetabular impingement, part II: midterm results of surgical treatment. *Clin Orthop Relat Res.* 2004;418:67–73
6. Byrd JW, Jones KS, Arthroscopic femoroplasty in the management of cam-type femoroacetabular impingement. *Clin Orthop Relat Res.* 2009;467:739–746
7. Caliesch R, Sattelmayer M, Reichenbach S, et al, Diagnostic accuracy of clinical tests for cam or pincer morphology in individuals with suspected FAI syndrome: a systematic review, *BMJ Open Sport Exerc Med,* 2020;6:e000772
8. Cooper RJ, *Geometric parameterisation in finite element models of femoroacetabular impingement,* 2017, [PhD Thesis] University of Leeds

9. Cooper RJ, Williams S, Mengoni M, et al., Patient-specific parameterised cam geometry in finite element models of femoroacetabular impingement of the hip. *Clin Biomec (Bristol Avon)*. 2018;54:62-70
10. Dessouky R, Chhabra A, Zhang L, et al., Cam-type femoroacetabular impingement—correlations between alpha angle versus volumetric measurements and surgical findings, *Eur Radiol*. 2019;29:3431–3440
11. Ellis SH, Perriman DM, Burns AWR, et al., Total volume of cam deformity alone predicts outcome in arthroscopy for femoroacetabular impingement, *Knee Surg Sports Traumatol Arthrosc*. 2020;28:1283–1289
12. Ganz R, Parvizi J, Beck M, et al., Femoroacetabular impingement: a cause for osteoarthritis of the hip, *Clin Orthop Relat Res*. 2003;417:112-20.
13. Grammatopoulos G, Speirs AD, Ng KCG, et al., Acetabular and spino-pelvic morphologies are different in subjects with symptomatic cam femoro-acetabular impingement, *J Orthop Res*. 2018;36:1840–1848
14. Griffin DR, Dickenson EJ, O'Donnell J, et al., The Warwick agreement on femoroacetabular impingement syndrome (FAI syndrome): an international consensus statement, *Br J Sports Med*. 2016;50:1169–1176
15. Griffin DR, Dickenson EJ, Wall PDH, et al., Hip arthroplasty versus best conservative care for the treatment of femoroacetabular impingement syndrome (UK FASHIoN): a multicentre randomised controlled trial, *Lancet* 2018;391: 2225–35.
16. Hatem M, Nimmons SJ, Khoury AN, et al., Spinopelvic parameters do not predict the sagittal orientation of the acetabulum, *Orthop J Sports Med*. 2020;8(10) 2325967120957420

17. Jones A (2022) Human hip joint impingement shape and motion model: input and output data for an initial study of eight typical cam-type hips. University of Leeds. [Dataset] <https://doi.org/10.5518/1231>
18. Kohnlein W, Ganz R, Impellizzeri FM, et al., Acetabular morphology implications for joint-preserving surgery, *Clin Orthop Relat Res.*, 2009;467:682–691
19. Krekel PR, Vochteloo AJH, Bloem RM, et al, Femoroacetabular impingement and its implications on range of motion: a case report, *J Med Case Rep*, 2011, 5:143
20. Lamontagne M, Kennedy MJ, Beaulé PE, The effect of cam FAI on hip and pelvic motion during maximum squat. *Clin Orthop Relat Res.* 2009;467:645–650.
21. Layton R. *Understanding movement and its influence on tribology of the human hip*. PhD Thesis. University of Leeds, 2020
22. Layton R, Messenger N, Stewart TD, Analysis of hip joint cross-shear under activities using a novel virtual joint model within Visual3D, *Proc Inst Mech Eng H.* 2021;235(10):1197-1204
23. Lerch TD, Boschung A, Todorski IAS, et al., Femoroacetabular impingement patients with decreased femoral version have different impingement locations and intra- and extraarticular anterior subspine FAI on 3D-CT-based impingement simulation: implications for hip arthroscopy, *Am J Sports Med.* 2019;47(13):3120–3132
24. Lubovsky O, Peleg E, Joskowicz L, et al., Acetabular orientation variability and symmetry based on CT scans of adults, *Int J Comput Assist Radiol Surg.* 2010;5:449-454
25. Mascarenhas VV, Castro MO, Rego PA, et al., The Lisbon agreement on femoroacetabular impingement imaging—part 1: overview, *Eur Radiol.* 2020;30:5281–5297

26. Mascarenhas VV, Rego P, Dantas P, et al., Hip shape is symmetric, non-dependent on limb dominance and gender-specific: implications for femoroacetabular impingement. A 3D CT analysis in asymptomatic subjects, *Eur Radiol.* 2018;28:1609–1624
27. Nakahara I, Takao M, Sakai T, et al., Gender differences in 3D morphology and bony impingement of human hips, *J Orthop Res.* 2011 Mar;29(3):333-9
28. Ng, K.C.G., Lamontagne, M., Labrosse, M.R., et al., Hip joint stresses due to cam-type femoroacetabular impingement: a systematic review of finite element simulations. *PLoS One.* 2016;11 (1): e0147813
29. Non-Arthroplasty Hip Registry. Available at: <https://www.nahr.co.uk/>. Accessed 17 May 2022.
30. Nordin & Frankel. *Basic Biomechanics of the Musculoskeletal System.* 3rd Edition, Lippincott Williams & Wilkins, 2001:204
31. Palmer AJR, Gupta VA, Fernquest S, et al., Arthroscopic hip surgery compared with physiotherapy and activity modification for the treatment of symptomatic femoroacetabular impingement: multicentre randomised controlled trial, *Br Med J.* 2019;364:1185
32. Pascual-Garrido C, Li DJ, Grammatopoulos G, et al., The pattern of acetabular cartilage wear is hip morphology-dependent and patient demographic-dependent, *Clin Orthop Relat Res.*, 2019;477:1021-1033.
33. Pierrepont J, Hawdon G, Miles BP, et al., Variation in functional pelvic tilt in patients undergoing total hip arthroplasty, *Bone Joint J.* 2017;99-B, No. 2
34. Savage TN, Saxby DJ, Pizzolato C, et al., Trunk, pelvis and lower limb walking biomechanics are similarly altered in those with femoroacetabular impingement syndrome regardless of cam morphology size, *Gait Posture.* 2021;83:26–34

35. Soames & Palastanga. *Anatomy and Human Movement*. 7th Edition, Elsevier, 2019:254
36. Steppacher SD, Lerch TD, Gharanizadeh K, et al., Size and shape of the lunate surface in different types of pincer impingement: theoretical implications for surgical therapy, *Osteoarthritis Cartilage*. 2014;22:951-958
37. Layton R, Messenger N, Stewart T (2022) Data Supporting Characteristics of hip joint reaction forces during a range of activities. [Dataset] <https://doi.org/10.5518/1253>
38. Leunig M, Beaulé PE, Ganz R, The concept of femoroacetabular impingement: current status and future perspectives, *Clin Orthop Relat Res.*, 2009;467:616-622.
39. Stull JD, Philippon MJ, LaPrade RF, “At-Risk” positioning and hip biomechanics of the Peewee ice hockey sprint start, *Am J Sports Med.*, 2011 Jul;39 Suppl:29S-35S
40. Sutter R, Dietrich TJ, Zingg PO, et al., How useful is the alpha angle for discriminating between symptomatic patients with cam-type femoroacetabular impingement and asymptomatic volunteers? *Radiology*, 2012;264(2):514-521.
41. Waterman BR, Ukwuani G, Clapp I, et al., Return to golf after arthroscopic management of femoroacetabular impingement syndrome, *Arthroscopy*. 2018;34(12):3187-3193.
42. Yun H, Murphy WS, Ward DM, et al., Effect of pelvic tilt and rotation on cup orientation in both supine and standing positions, *J Arthroplasty*. 2018;33:1442-1448